Zebrafish *vasa* RNA but Not Its Protein Is a Component of the Germ Plasm and Segregates Asymmetrically before Germline Specification

Holger Knaut,* Francisco Pelegri,* Kerstin Bohmann,* Heinz Schwarz,‡ and Christiane Nüsslein-Volhard*

*Max Planck Institut für Entwicklungsbiologie Abteilung Genetik, ‡Elektronenmikroskopie Labor, 72076 Tübingen, Germany

Abstract. Work in different organisms revealed that the *vasa* gene product is essential for germline specification. Here, we describe the asymmetric segregation of zebrafish *vasa* RNA, which distinguishes germ cell precursors from somatic cells in cleavage stage embryos. At the late blastula (sphere) stage, *vasa* mRNA segregation changes from asymmetric to symmetric, a process that precedes primordial germ cell proliferation and perinuclear localization of Vasa protein. Analysis of hybrid fish between *Danio rerio* and *Danio feegradei* demonstrates that zygotic *vasa* transcription is initiated shortly after the loss of unequal *vasa* mRNA segregation. Blocking DNA replication indicates that the change in *vasa* RNA segregation is dependent on a maternal program. Asymmetric segregation is impaired in embryos mutant for the maternal effect gene *nebel*. Furthermore, ultrastructural analysis of *vasa* RNA particles reveals that *vasa* RNA, but not Vasa protein, localizes to a subcellular structure that resembles nuage, a germ plasm organelle. The structure is initially associated with the actin cortex, and subsequent aggregation is inhibited by actin depolymerization. Later, the structure is found in close proximity of microtubules. We previously showed that its translocation to the distal furrows is microtubule dependent. We propose that *vasa* RNA but not Vasa protein is a component of the zebrafish germ plasm. Triggered by maternal signals, the pattern of germ plasm segregation changes, which results in the expression of primordial germ cell–specific genes such as *vasa* and, consequently, in germline fate commitment.

Key words: primordial germ cells • *Danio rerio* • *nebel* • asymmetric segregation • RNA localization

Introduction

Asymmetric cell division contributes to the generation of cell diversity in many organisms (for reviews see Horvitz and Herskowitz, 1992; Rhyu and Knoblich, 1995; Knoblich, 1997; Jan and Jan, 1998, 1999). One way to achieve asymmetric cell division is to unequally partition intrinsic cell fate determinants from the mother cell to only one of the two daughter cells. Such a mechanism is used in mating type switching in yeast (Bobola et al., 1996; Sil and Herskowitz, 1996; Long et al., 1997; Takizawa et al., 1997), in *Drosophila* and vertebrates during neurogenesis (Rhyu et al., 1994; Hirata et al., 1995; Knoblich et al., 1995; Spana and Doe, 1995; Spana et al., 1995; Shen et al., 1998; Schober et al., 1999; Wodarz et al., 1999), and in germline specification in *Caenorhabditis*, *Drosophila*, and *Xenopus* (Nieuwkoop and Sutasurya, 1979; Rongo et al., 1997; Seydoux and Strome, 1999).

In *Caenorhabditis* and *Drosophila*, germline determinants are asymmetrically localized as components of a special type of cytoplasm, the germ plasm (for reviews see Rongo et al., 1997; Seydoux and Strome, 1999). This cytoplasm consists of electron-dense material in association with fibrils, mitochondria, and often the nuclear envelope. Because of its cloudy appearance in ultrastructural studies, it has been termed nuage (Andre and Rouiller, 1957). In *Drosophila*, nuage is first detected in nurse cells, and it is thought to represent the precursor of polar granules (Mahowald, 1968, 1971; Eddy, 1975). During oogenesis, the polar granules are recruited to the posterior of the oocyte and form the germ plasm (called pole plasm). Upon pole cell formation, the granules fragment and associate with the outer nuclear envelope as nuage and remain associated with the germ cells throughout the life cycle of the *Drosophila* (Mahowald, 1962, 1968, 1971). Similarly, germline cells in *Caenorhabditis*, *Xenopus*, and zebrafish also are characterized by nuage-like structures that segregate

Address correspondence to Holger Knaut, Max Planck Institut für Entwicklungsbiologie Abteilung Genetik, Spemannstrasse 35, 72076 Tübingen, Germany. Tel.: 49-7071-601-490. Fax: 49-7071-601-384. E-mail: holger.knaut@tuebingen.mpg.de

The present address of F. Pelegri is Laboratory of Genetics, University of Wisconsin-Madison, 445 Henry Mall, Madison, WI 53706-1574.

to the primordial germ cells (PGCs)[1] and, again, remain associated with the germline throughout development (Eddy, 1975; Selman et al., 1993; Braat et al., 1999; Seydoux and Strome, 1999).

Transplantation experiments in *Drosophila* and *Xenopus* together with genetic studies in *Drosophila* and *Caenorhabditis* demonstrate that germ plasm is required for germ cell induction (Illmensee and Mahowald, 1974; Okada et al., 1974; Nieuwkoop and Sutasurya, 1979; Ephrussi et al., 1991; Ephrussi and Lehmann, 1992; Seydoux and Strome, 1999) and, in the case of *Drosophila* and *Caenorhabditis*, leads to transcriptionally silenced nuclei (Zalokar, 1976; Seydoux and Dunn, 1997; Asaoka et al., 1998; Van Doren et al., 1998). Yet, the time point at which germline specification occurs is different among these species. In *Drosophila* and *Caenorhabditis*, the germline is separated from the somatic tissue immediately at the onset of embryogenesis, whereas, in *Xenopus*, restriction to the germline occurs shortly before gastrulation (for review see Wylie, 1999). In fish, the specification of germ cells is poorly understood. Nuage-like structures are detected during oogenesis and late embryogenesis, and the origin of germ cells has been traced to different germ layers in different fish (Hamaguchi, 1982; Wallace and Selman, 1990; Gevers et al., 1992; Selman et al., 1993; Braat et al., 1999). Therefore, it is difficult to assign a specific time point and event to germ cell specification in fish.

The recent identification of the zebrafish *vasa* orthologue indicates that germ cell precursors are separated early from somatic cells, and they can be traced throughout embryogenesis (Olsen et al., 1997; Yoon et al., 1997; Weidinger et al., 1999; Braat et al., 1999). The *vasa* gene was initially identified in *Drosophila* by genetic screens for maternal-effect mutations that affect anterior–posterior polarity. Embryos from mutant mothers lack localized polar granules and do not form pole cells (Schüpbach and Wieschaus, 1986; Lehmann and Nüsslein-Volhard, 1991). The *vasa* gene encodes an RNA helicase of the DEAD box family (Hay et al., 1988b; Lasko and Ashburner, 1988) that is expressed specifically in the germline throughout the life cycle (Lasko and Ashburner, 1990). In oocytes, *vasa* RNA is uniformly distributed in the cytoplasm, whereas the protein associates with polar granules and is asymmetrically segregated to the posterior pole (Hay et al., 1988a). After pole cell formation, *vasa* protein is exclusively found in the germline. The expression of the two *vasa* homologues in *Caenorhabditis* (glh-1 and glh-2) is similar. The Vasa proteins are associated with the P granules, which are asymmetrically segregated to the germline precursors and restricted to the germline throughout the life cycle (Gruidl et al., 1996). Vertebrate *vasa* homologues have been identified and shown to be expressed in the germline at later stages of embryogenesis (Fujiwara et al., 1994; Komiya et al., 1994; Komiya and Tanigawa, 1995). In zebrafish, *vasa* RNA is found throughout oogenesis and embryogenesis (Olsen et al., 1997; Yoon et al., 1997; Braat et al., 1999). Strikingly, the *vasa* transcript is localized to the distal parts of the first two cleavage furrows as granules and eventually ingresses into four cells of the blastula. The number of *vasa* RNA–positive cells remains constant until the sphere stage (cell cycle 13; all staging is according to Kimmel et al., 1995), where *vasa* RNA–positive cells increase in number and migration to the gonads begins. Recent studies have demonstrated that these cells are presumably the zebrafish PGCs because of their migration pattern, final location and morphology (Olsen et al., 1997; Yoon et al., 1997; Braat et al., 1999; Weidinger et al., 1999).

Initial insights into the mechanism of early zebrafish vasa RNA localization came from microtubule inhibition studies. Embryos treated with the microtubule depolymerizing reagent nocodazole fail to translocate *vasa* RNA to the distal cleavage planes, a phenotype that is also observed in the maternal-effect mutation *nebel* (Pelegri et al., 1999). Embryos from homozygous *nebel* mutant mothers (referred to as *nebel* embryos) have reduced furrow-associated microtubule and cellularization defects (Pelegri et al., 1999). However, the nature of these localized *vasa* RNA structures, their mode of assembly, and restriction to a limited number of cells and the time point of germ cell specification have not yet been resolved.

In this paper, we show that *vasa* RNA is a component of a germ plasmlike structure. We also show that *vasa* RNA segregates asymmetrically to the future founder population of PGCs. The asymmetric segregation is impaired in embryos mutant for the maternal-effect gene *nebel*. We find that a change in *vasa* RNA localization at the sphere stage (cell cycle 13) precedes PGC proliferation, Vasa protein localization, and zygotic *vasa* transcription. This transition is independent of zygotic or nuclear signals, suggesting that maternal signals induce a change in germ plasm segregation, which results in germ plasm activation and consequently in germline specification.

Materials and Methods

cDNA Cloning

Poly(A)$^+$ RNA was enriched from the 4-cell stage *D. rerio* and *D. feegradei* embryos using TriStar Reagent (Angewandte Gentechnologie Systeme) and oligotex columns (Qiagen) according to the manufacturer's instructions. First strand cDNA synthesis was performed using Superscript II (Gibco-BRL Life Sciences) with the primer 5′-CCAGTGAGCAGAGTGACGAGGACTCGAGCTCAAGCTTTTTTTTTTTTTT-TTBN-3′. The 3′ untranslated region (UTR) of *D. rerio vasa* was amplified with the primers 5′-CCGGCTCGAGCTGGCCTCACACCT-3′ and 5′-GGCCTCTAGAGTCACCAGTATCCGTC-3′ and *Taq* polymerase (Amersham Pharmacia Biotech; 94°C for 30 s, 60°C for 1 min, 72°C for 90 s and 25 amplification cycles). The 3′ UTR of *D. feegradei vasa* was amplified by 3′RACE with two primer pairs: 5′-CCAGTGAGCAGAGTGACG-3′ and 5′-AGTCTGAGCACACGCCAT-3′, and 5′-GAGGACTCGAGCTCAAGC-3′ and 5′-GAAGGCCGCCGTTTTTCC-3′ using *Taq* polymerase (Amersham Pharmacia Biotech; 94°C for 1 min, 58°C for 1 min, 72°C for 3 min and 30 amplification cycles). Sequence alignment was performed using Lasergene software (DNAStar).

Whole-mount In Situ Hybridization and Antibody Stainings

For Vasa protein stainings, embryos were fixed in Dent's fixative (80% methanol and 20% DMSO) at –20°C overnight. After rehydration and dechorionation, embryos were blocked in PBS with 0.2% Triton X-100 and 1% BSA (PBTB) for 1 h at room temperature, incubated with the pri-

[1]*Abbreviations used in this paper:* dpf, days post fertilization; FMA, furrow microtubule array; hpf, hours postfertilization; MBT, midblastula transition; PGC, primordial germ cell; RACE, rapid amplification of cDNA ends; RNAPII, RNA polymerase II; UTR, untranslated region.

mary antibody (anti-*vasa* K12-3) at a 1:5,000 dilution in PBTB at 4°C overnight, washed with PBTB four times for 20 min, incubated with the secondary antibody (goat anti–rabbit IgG coupled to alkaline phosphatase, Cy5, FITC, or Cy3, Dianova) for 2 h at room temperature, and washed with PBT four times for 20 min. For Vasa protein stainings at the sphere (cell cycle 13) to dome stage (cell cycle 13–14), a tertiary donkey anti–goat Cy3-conjugated antibody was used to enhance the fluorescence signal (Dianova). Alkaline phosphatase detection was done as described in Ober and Schulte-Merker (1999). For double staining of Vasa protein and the nuclear membrane, embryos were treated as above but anti–lamin B antibody was added to the primary antibody incubation step (Pugh et al., 1997; Dahm et al., 1998) and detected with goat anti–mouse IgG Cy3 coupled to (Dianova). For colocalization of *vasa* RNA and Vasa protein, in situ hybridization was performed as described in Ober and Schulte-Merker (1999), with the exception that goat anti–digoxigenin coupled to HRP (Boehringer Mannheim) was used, and the staining was done as described in Hopman et al. (1998). Immunodetection of Vasa protein in stained embryos was performed as described above. For double and triple detection of *vasa* RNA and β-catenin, RNA polymerase II, nuclear pore complexes and/or γ-tubulin, the embryos were stained for *vasa* RNA and proteins as described above using the mouse mAbs anti–β-catenin, anti–γ-tubulin (Sigma-Aldrich), mAb 414 (Hiss Diagnostics), and H5/H14 (Hiss Diagnostics) at a dilution of 1:1,000. Colocalization of α-tubulin and *vasa* RNA was done as described in Pelegri et al. (1999) with the modification that 0.0025% glutaraldehyde and 5 mM magnesium sulfate were used in the fixation step. The dimeric cyanine nucleic acid stain 3 (TOTO-3) and propidium iodide (Molecular Probes) were used for nuclear staining. *vasa* RNA probes were synthesized from the 3′ UTR of *D. rerio* and *D. feegradei* (corresponding to nucleotides 2,222–2,865 of *vasa* cDNA from *D. rerio*, accession number AB005147; and nucleotides 1,153–1,779 of *vasa* cDNA form *D. feegradei*, accession number AF251800). For visualization, a Leica TS system confocal microscope was used.

Antibody Generation

The COOH-terminal part of the Vasa protein (amino acids 544 to stop) was cloned into pRSETA (Invitrogen Corp.) to generate a His-tagged fusion protein. The fusion protein was overexpressed in *Escherichia coli* and was purified on nickel agarose columns (Qiagen). The purified protein was mixed with 1 vol of Freund's adjuvant (Sigma-Aldrich), and 500 μg of protein was used for immunization of rabbits. After the initial immunization, rabbits were boosted and bled in 2-wk intervals. Antibody titer was checked on Western blots. Batches of antisera were partially affinity-purified against His-tagged fusion protein immobilized on Sepharose-CNBr–activated columns (Amersham-Pharmacia). For Western blot analysis, affinity-purified K12-3 antiserum was used (1:2,000), whereas whole-mount stainings were done with the crude antisera K12-3 (1:5,000 or 1:10,000).

Electron Microscopy

For *vasa* RNA and protein detection on electron microscopy sections, embryos were stained as described above with the modification that the proteinase K step was omitted in the case of in situ hybridization. The signal was detected using DAB (Boehringer Mannheim). For structural electron microscopy sections, embryos were fixed in 1% glutaraldehyde and 4% paraformaldehyde in PBS and freeze-substituted in Epon 812 (Roth). All sections were contrasted using uranylacetate and osmium tetroxide and inspected using a Philips TEM 10 electron microscope.

Drug Treatment of Embryos

Latrunculin B (BioMol Research Laboratories) was prepared as a stock solution of 3 mg/ml in DMSO and used at a concentration of 30 μg/ml diluted in distilled water. Single cell embryos were coinjected with 50 nl of the indicated concentration and phenol red as a marker. Aphidicolin (Sigma-Aldrich) was dissolved in 50% DMSO at a concentration of 2.5 mg/ml. For injections, the aphidicolin stock was diluted 1:10 in distilled water and 50 nl was injected in single cell embryos. Actinomycin D (Sigma-Aldrich) was dissolved at a concentration of 5 mg/ml in water and 50 nl of a 1:1,000 dilution in distilled water was injected in single cell embryos. As controls, embryos were injected with the same amount of the solvent. Embryos were stained for *vasa* RNA by in situ hybridization as described above.

Fish Maintenance and Mutant Strain

Zebrafish were maintained as previously described (Mullins et al., 1994; Haffter et al., 1996). For all experiments, the Tübingen and TL strain were used. *nebel* mutants were kept in the TL background. No difference between the Tübingen and TL strain was observed, although a difference in primordial germ cell number was reported for the AB strain (Weidinger et al., 1999).

Determination of Germ Plasm–containing Cells

Germ plasm–containing cells were determined by *vasa* RNA and/or protein expression using a stereomicroscope or a fluorescence microscope. Since the number of germ plasm–containing cells varied, embryos were taken from the same clutch during a particular time course analysis.

Generation of *D. rerio*–*D. feegradei* Hybrid Fish and Detection of Zygotic Vasa Transcription

To generate hybrid fish, *D. rerio* eggs were in vitro fertilized with *D. feegradei* sperm, which was isolated from the testes as described in Pelegri and Schulte-Merker (1999). Hybrid embryos were collected for cDNA preparation and fixed for protein and RNA stainings as described above. As controls, *D. rerio* and *D. feegradei* embryos were collected in the same manner. Genomic DNA from both fish species was prepared as described in Yoon et al. (1997). Specific primers for *vasa* cDNAs from both species were designed such that genomic contamination in the cDNA preparation was detected by the presence of an intron. For *D. feegradei*, the primer pair 5′-CTGCCATCCTACAGAGA-3′ and 5′-CATCACTGCATGCTCCACC-3′, and, for *D. rerio*, the primer pair 5′-TTGTTCAGGTGGACCAGTAC-3′ and 5′-GGGCAGATGTTTGTGATGGT-3′ were used. Detection of *vasa* transcripts was performed using *Taq* polymerase (Amersham-Pharmacia; 94°C for 30 s, 60°C for 30 s, 73°C for 1 min and 35 amplification cycles).

Results

vasa RNA Is a Component of Zebrafish Germ Plasm

To understand the structural nature of localized *vasa* RNA aggregates in zebrafish embryogenesis, we performed transmission electron microscopy on four-cell embryos that are labeled for *vasa* RNA using in situ hybridization and an electron-dense substrate (see Materials and Methods). Ultrathin sections of these embryos show that the transcript is restricted to a distinct, electron-dense structure, which is in close proximity to the indented furrow (Fig. 1, a and b). The densely labeled structure consists of porous elements embedded in an electron-dense matrix and resembles nuage-like structures found associated with germ cells and their precursors in many animals (Eddy, 1975). To investigate whether *vasa* RNA remains associated with these nuage-like structures in PGCs, we analyzed sections of embryos at later stages. We found *vasa* RNA to be associated with the same nuage-like structures in the 1,000-cell stage embryos (Fig. 1, c and d). In the 2.5-d postfertilization (dpf) embryos, we failed to detect *vasa* RNA in Vasa protein–positive cells (data not shown), presumably because of the too low *vasa* RNA transcript levels as judged by Northern analysis (Yoon et al., 1997, and our own observations). Based on the presence of the *vasa* RNA, which is embedded in electron-dense material that resembles nuage, we conclude that this structure is the zebrafish germ plasm.

Germ Plasm First Associates with the Actin Cortex, and then with the Microtubule Network

Because of the harsh nature of the in situ technique, few cytoplasmic structures are conserved around the nuage-like structures (Fig. 1, a–d). Therefore, we decided to section

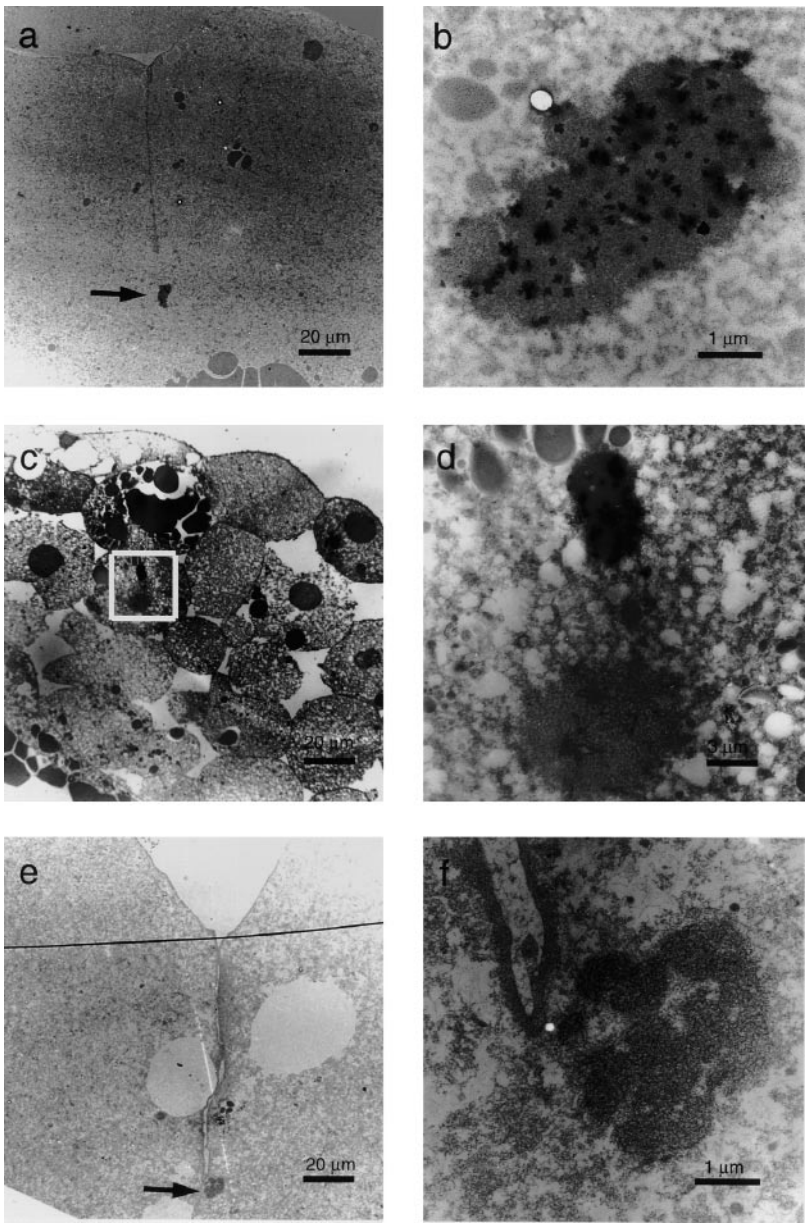

Figure 1. Electron microscopy sections of 4-cell (a, b, e, and f) and 1,000-cell (c and d) embryos stained for *vasa* RNA. Embryos were hybridized with antisense (a–d) and sense (e–f) *vasa* RNA fragments, embedded, and processed for electron microscopy. All sections are along the animal-vegetal axis. *vasa* RNA is confined to a structure vegetal to the indented furrow (arrow in a and magnified in b). Serial sections show that this structure is 2–5 μm in width and 4–8 μm in length. The structure is also detectable in the 1,000-cell stage embryos (white square in c and magnified in d). This structure is specifically stained by antisense *vasa* RNA (arrow in a and magnified in b) but not with sense *vasa* RNA (arrow in e and magnified in f).

structurally preserved embryos to analyze germ plasm in a more natural context. Before aggregation of germ plasm at the distal ends of the first cleavage furrow, we always find nuage-like structures evenly distributed in small particles of 1 μm in diameter adjacent to or in the proximity of the actin cortex (Fig. 2 a). After aggregation in two- and four-cell embryos, the nuage-like particles have increased in size and form rodlike structures underneath the incomplete furrow. These aggregated particles are no longer seen in proximity to the actin cortex, but rather are seen in close association with microtubule and mitochondria (Fig. 2, b and c). Some small particles are still detected along the actin cortex, though fewer in number.

Since germ plasm particles are found close to the actin cortex in single cell embryos, we asked whether actin plays a role in initial germ plasm aggregation. To test this hypothesis, we treated single cell embryos with latrunculin B, an actin inhibitor (Spector et al., 1983). The treated embryos failed to aggregate germ plasm particles. Instead, we see germ plasm around the edges of the cortex (data not shown) and no accumulation at the cleavage planes. This observation is consistent with the idea that the initial aggregation of the germ plasm is actin dependent. However, we cannot exclude a secondary effect of actin inhibition on germ plasm aggregation since this agent also inhibits the formation of the cellular furrow (Rappaport, 1996).

Vasa Protein Distribution during Oogenesis and Embryogenesis

The observation that zebrafish *vasa* RNA is localized to the germ plasm raised the question whether Vasa protein is also a germ plasm component. To test this possibility, we raised rabbit anti-Vasa antibodies to characterize the subcellular distribution of Vasa protein during oogenesis and embryogenesis. The antiserum detects a band of 80 kD on

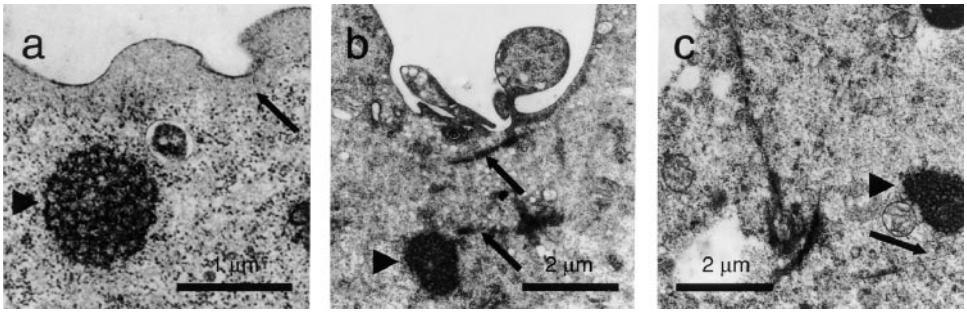

Figure 2. Ultrastructural analysis of zebrafish germ plasm. Embryos were fixed, embedded, and processed for electron microscopy. All sections are along the animal-vegetal axis. In the 1-cell stage embryos, the germ plasm (arrowhead) is scattered in little patches that are in direct physical contact or close proximity to the indicated cortical actin network (a). After furrow initiation, these patches of germ plasm aggregate underneath the forming furrow and are seen in close proximity to microtubule bundles (b). After a second furrow indentation, the germ plasm aggregates are seen vegetal to the furrow, again in close proximity to bundles of microtubules (c). Arrows indicate actin cortex (a) and microtubule (b and c).

a Western blot, which is consistent with the calculated molecular mass of 77 kD (see Fig. 4 e). The preimmune rabbit serum does not cross-react with fish proteins of similar size. Anti-Vasa antibody–depleted serum fails to detect both the 80-kD Western band and primordial germ cells in whole-mount antibody staining (data not shown). We conclude that the anti-Vasa antibody is specific for Vasa protein.

In whole-mount double stainings for *vasa* RNA and the protein of stage I oocytes, *vasa* RNA is diffuse and cytosolic, whereas the protein is localized in patches around the germinal vesicle (Fig. 3, a and b). In stage II oocytes, *vasa* RNA is transiently localized to the cytosolic part of cup-shaped granules, presumably cortical granules, and then accumulates around the animal cortex of the maturing oocyte (Fig. 3 c). Vasa protein remains associated with the germinal vesicle until germinal vesicle breakdown between stage III and IV (Fig. 3, d and e). During late oogenesis, we detect uniform Vasa protein presumably because of its cytoplasmic localization. We cannot detect localized Vasa protein by whole-mount stainings before the late sphere (cell cycle 13) stage, although developmental Western analyses suggest that the protein is present at equivalent levels throughout embryogenesis (Fig. 4 e). In stainings at these early stages, Vasa protein shows a diffuse cytoplasmic distribution, suggesting that the maternal Vasa protein is neither localized nor confined to a subpopulation of cells (data not shown). Beginning at the sphere (cell cycle 12–13) stage, Vasa protein–positive cells display the same migration pattern as shown with in situ stainings against *vasa* RNA, suggesting colocalization of Vasa protein and RNA to the same cell population. Vasa protein is detected as a faint perinuclear staining in four clusters of one to four cells each in late sphere stage embryos (cell cycle 13; Fig. 4 a). Beginning at the dome stage (cell cycle 13–14), Vasa protein–positive cells can be followed

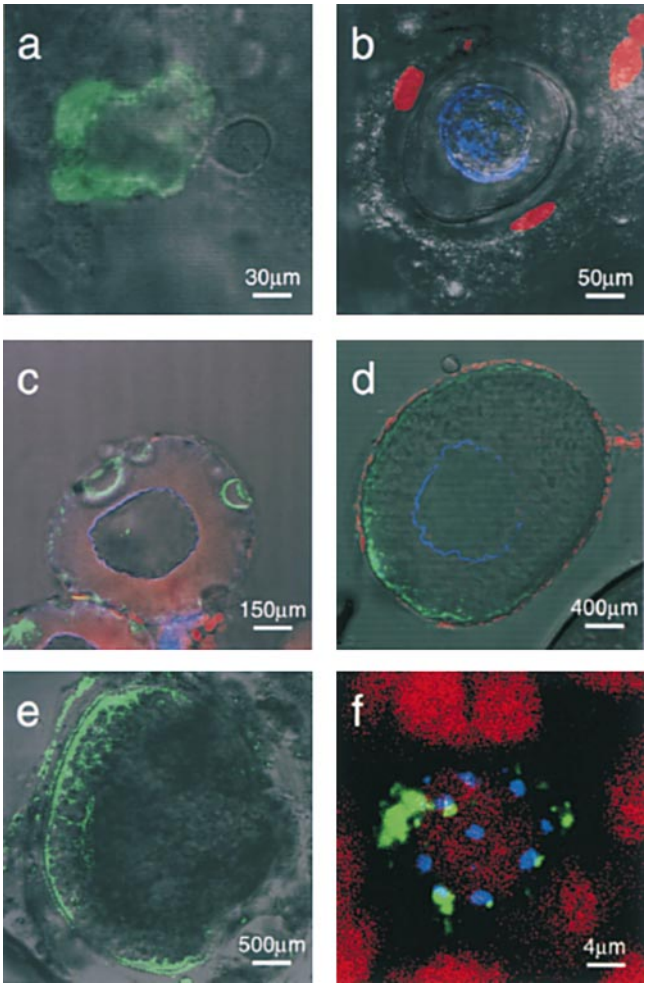

Figure 3. vasa RNA and protein distribution during oogenesis (a–e, animal pole to the left) and embryogenesis (f). Oocytes were hybridized with antisense *vasa* RNA fragments (green) and stained for Vasa protein (blue), except in Fig. 3 (a and b) where single staining was performed. Follicle cell nuclei were visualized with the nuclear dye propidium iodide (red) that does not stain oocyte nuclei. Stainings were analyzed by confocal microscopy and superimposed with DIC images. In stage I oocytes, vasa RNA is cytoplasmic (a), whereas Vasa protein is localized around the germinal vesicle (b). Later in stage II oocytes, the RNA localizes to cortical cuplike structures while the Vasa protein remains associated with the germinal vesicle (c). In stage III oocytes, vasa RNA enriches at the animal pole cortex (d). After germinal vesicle breakdown between stages III and IV, Vasa protein localization is lost while the RNA remains cortical (e). In 30 hpf embryos, vasa RNA is found in patches within the cytosol again and the protein resumes its perinuclear location (f).

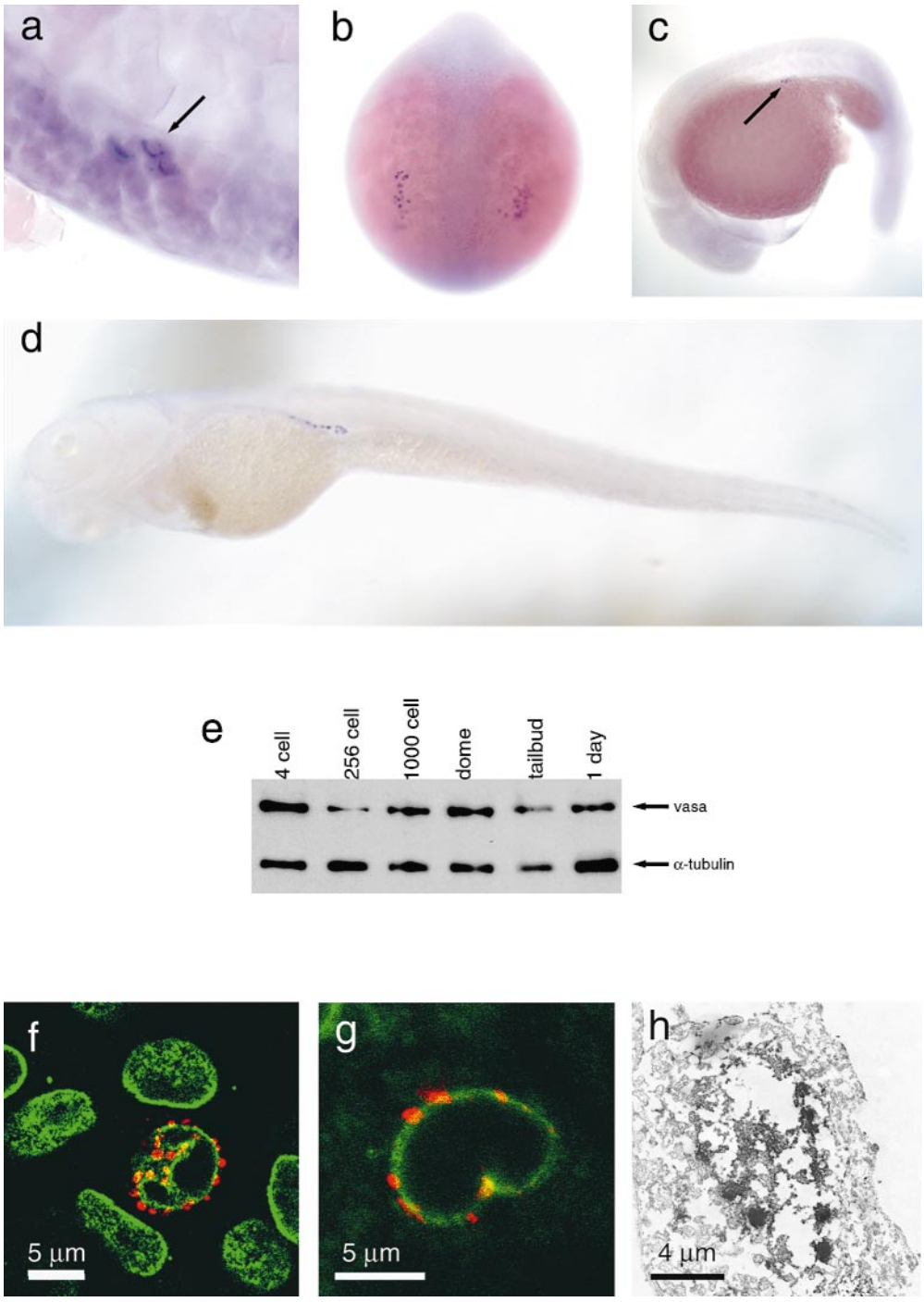

Figure 4. Vasa protein expression during early zebrafish development. Whole-mount anti-vasa antibody stainings (a–d) detect localized vasa protein expression beginning at the sphere stage (a, arrow). The Vasa protein–positive cells migrate, and are found in two clusters of roughly 15 cells each at the 6 somite stage (b). After 1 dpf, the two clusters of Vasa protein–positive cells are found at the anterior of the yolk extension (c) and later at 3 dpf these clusters are just posterior of the forming swim bladder (d). Developmental Western analysis shows that the Vasa protein is maternally provided (e). Total protein from embryos at various developmental stages was blotted and probed with affinity-purified anti-vasa antibody K12-3. The developmental stages are indicated and equal amounts of protein (0.5 embryos per slot) were loaded as judged by the amounts of α-tubulin. Subcellular localization of Vasa protein was analyzed by confocal and electron microscopy in 30 hpf embryos (f–h). For confocal microscopy, the embryos were stained for Vasa protein (red) and lamin B (green in f), nuclear pore complexes (green in g). Embryos for ultrastructural analysis were stained for Vasa protein and detected with DAB. Both stainings (f and h) show that vasa protein is tightly associated with the nuclear envelope. The protein accumulates in tight, perinuclear spots that are evenly spaced and are not enriched in nuclear pore complexes (g).

throughout embryogenesis, as they migrate to form two clusters lateral to the paraxial mesoderm extending roughly from somites 2–4 at the 6 somite stage (Fig. 4 b). At 24 hpf, the Vasa protein–positive cells are located in two clusters at the anterior part of the yolk extension, from where they extend posteriorly in two bilateral rows of cells dorsolateral to the forming gut (Fig. 4, c and d).

To address the structural nature of the perinuclear localization of Vasa protein and its possible colocalization with *vasa* RNA, we analyzed the Vasa protein distribution on its own and together with *vasa* RNA in 30 hpf embryos. Vasa protein is localized strictly perinuclear to granules. These granules do not colocalize with the nuclear pore as has been reported for *Caenorhabditis* (Pitt et al., 2000), and are distinct from *vasa* RNA–containing structures (Fig. 4, f–h). *vasa* RNA is partially perinuclear, partially cytosolic, and does not colocalize with Vasa protein (Fig. 3 f), a pattern reminiscent of what is seen at early oogenesis. From these observations, we draw two conclusions. First, we infer that Vasa protein is not a component of the zebrafish germ plasm. Second, we believe that while *vasa* RNA is subcellularly localized to the distal cleavage fur-

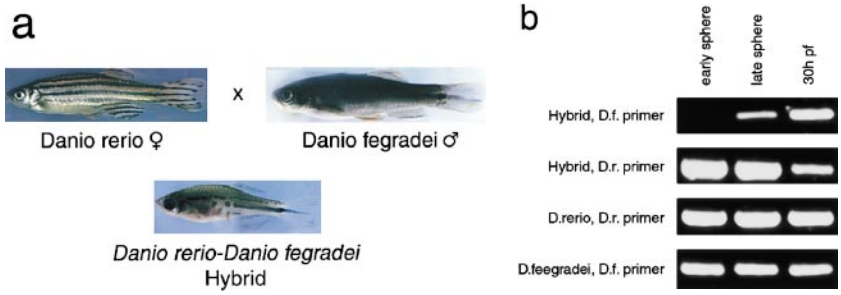

Figure 5. Detection of zygotic *vasa* RNA transcripts. *D. rerio–D. feegradei* hybrid fish were generated by in vitro fertilization (a). Determination of zygotic *vasa* transcription was performed as described. *D. feegradei*–specific *vasa* primers fail to amplify *vasa* in *D. rerio–D. feegradei* hybrids until the late sphere stage, whereas they amplify *vasa* throughout embryogenesis in *D. feegradei*. *D. rerio*–specific *vasa* primers amplify *vasa* in both *D. rerio–D. feegradei* hybrids and *D. rerio* throughout embryogenesis (b). Amplified genomic *vasa* DNA can be distinguished from *vasa* cDNA by intronic sequences induced band shifts (data not shown).

rows during early cell divisions (Olsen et al., 1997; Yoon et al., 1997; and our own observations), its protein remains in all cells. The accumulation of Vasa protein in PGCs at the late sphere stage (cell cycle 13) may, therefore, occur by de novo synthesis. Alternatively, perinuclear Vasa protein accumulation also could reflect active recruitment of maternal protein.

Zygotic vasa Transcription Starts at Late Sphere Stage (Cell Cycle 13)

To resolve the question of the initial origin of perinuclear-localized Vasa protein at the late sphere stage (cell cycle 13), we analyzed the onset of zygotic transcription of *vasa* RNA. To this end, we devised a strategy that allowed us to monitor zygotic *vasa* RNA in the background of maternal *vasa* RNA. First, we cloned the *vasa* homologue of *D. feegradei*, a fish closely related to *D. rerio* (data not shown; accession number AF251800). Based on polymorphism in the 3′ UTR of these two species, we designed primers that are specific for either *vasa* transcript (data not shown and Fig. 5 b). Then, we created hybrid embryos from *D. rerio* females and *D. fegradei* males by in vitro fertilization (Fig. 5 a) and used reverse transcriptase–PCR to follow the initiation of paternal (i.e., zygotic) *vasa* transcription during development. The localization pattern of *vasa* RNA and early embryogenesis of *D. feegradei* and the *D. rerio–D. feegradei* hybrids resembles *D. rerio* (data not shown), and, therefore, it is likely that both species utilize similar mechanisms for this process. Our reverse transcriptase–PCR approach demonstrates that whereas we are able to amplify maternal *vasa* RNA throughout early embryogenesis, paternal (i.e., zygotic) *vasa* RNA is first detectable at the late sphere stage (cell cycle 13; Fig. 5 b). Therefore, zygotic *vasa* expression is initiated shortly after the beginning of general zygotic transcription. The activation of the *vasa* promoter at the late sphere stage (cell cycle 13) suggests that PGCs adopt their fate at the onset of their proliferation and migration period.

To analyze the relationship between the onset of zygotic *vasa* transcription and localized Vasa protein, we determined the Vasa protein distribution in embryos at the early sphere stage (cell cycle 12–13), which do not yet express zygotic *vasa* (early sphere stage, cell cycle 12–13). Only a few embryos within such a clutch show Vasa protein accumulation in the four to five presumptive PGCs. In contrast, all embryos at the dome stage (cell cycle 13–14), which have begun transcribing *vasa* RNA, show Vasa protein accumulation in these four to five cells (data not shown). These observations suggest that translation of maternal RNA provides a minor contribution to the localized Vasa protein, and that further Vasa protein accumulation relies on translation of zygotically expressed *vasa* RNA. In support of this observation, we also find weak Vasa protein accumulation in four to five cells in the late sphere stage (cell cycle 13) embryos lacking genomic DNA and, hence, zygotic *vasa* contribution (see below).

Germ Plasm Does Not Transcriptionally Silence the Nucleus

Although the activation of the zygotic genome at mid-blastula transition (MBT) occurs at 3.0 hpf (Kane and Kimmel, 1993), our experiments indicate that zygotic *vasa* transcription occurs approximately 1 h later, at ~4.0 hpf (Fig. 5 b). This prompted us to ask whether presumptive germ cell nuclei are, in general, transcriptionally quiescent until the sphere stage (cell cycle 13). Transcriptional quiescence has been reported for germ cell nuclei of *Drosophila* and *Caenorhabditis* (Zalokar, 1976; Seydoux and Dunn, 1997; Asaoka et al., 1998; Van Doren et al., 1998). To address this question, we used the H5 mAb. This antibody specifically recognizes a phosphoepitope on the COOH-terminal domain of the RNA polymerase II (RNAPII). This epitope has been reported to reflect elongating and, thus, transcriptionally active RNAPII, and is a marker for actively transcribing nuclei (Warren et al., 1992; Bregman et al., 1995; Kim et al., 1997; Seydoux and Dunn, 1997; Patturajan et al., 1998). No RNAPII signal is detected with the H5 antibody in the nuclei of 128-cell stage embryos (Fig. 6 a), although we see an RNAPII signal with the H14 mAb that recognizes a phosphoepitope that does not correlate with transcriptional activity in extracts of pre- and post-MBT embryos (Fig. 6 c). Shortly before MBT, at the transition from the 256- to 512-cell stage, we see distinct subnuclear staining of cells containing and lacking germ plasm with the H5 antibody that persists at least until late epiboly (Fig. 6 b and data not shown). Since we can detect no difference between cells with and without germ plasm in H5 RNAPII stainings, we suggest that transcription is initiated at MBT in all nuclei irrespective of germ plasm.

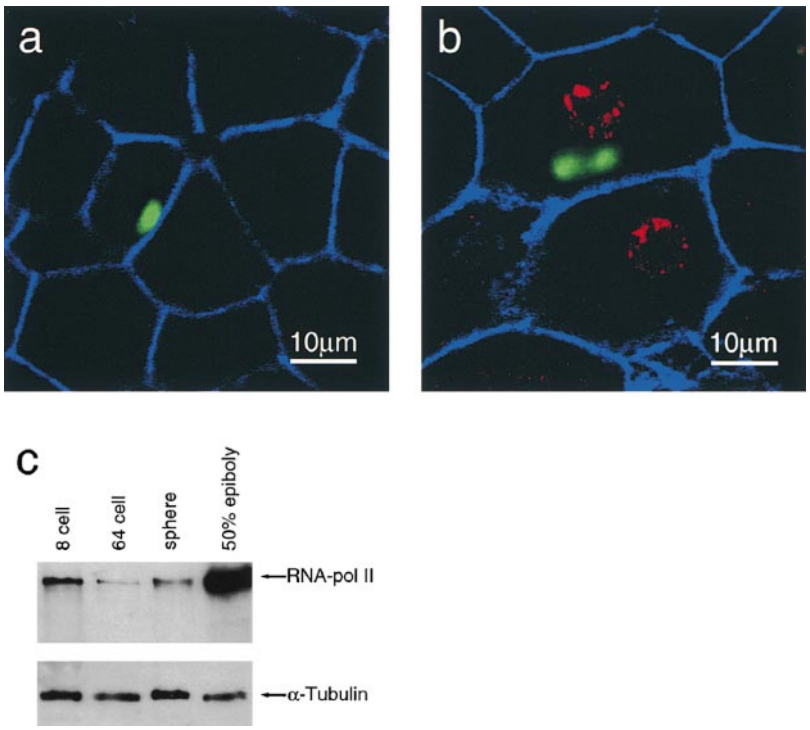

Figure 6. Transcriptional activity in presumptive PGCs during embryogenesis. Embryos were stained for *vasa* RNA (green), β-catenin (blue), and an elongation-specific phosphoepitope of RNAPII (red) with the mAb H5 (a and b). In the 128-cell stage embryos, we failed to detect any H5-positive nuclei (a). The signal is first detectable at the 256-cell stage when nuclei express the H5 elongation–specific RNAPII epitope irrespective of *vasa* RNA–containing germ plasm (b). Developmental Western analysis shows that RNAPII is present throughout early embryogenesis (c). Total protein from embryos at various developmental stages was blotted and probed with the mAb H14 that recognizes a ubiquitous phosphoepitope of RNAPII. The developmental stages are indicated, and equal amounts of protein (0.5 embryos per slot) were loaded as judged by the amounts of α-tubulin.

Germ Plasm Is Initially Asymmetrically, and then Symmetrically Segregated into Daughter Cells

We were interested in the reasons why the number of presumptive PGCs remains constant during initial cleavages while somatic cells increase dramatically in number. There are two possibilities to account for the lack in primordial germ cell proliferation until the sphere stage (cell cycle 13): either germ plasm–containing cells do not divide during early embryogenesis, as has been shown for *Drosophila*, or germ plasm is segregated asymmetrically to one daughter cell during cell division, as has been reported for *Caenorhabditis* and *Xenopus* (Whitington and Dixon, 1975; Seydoux and Strome, 1999) and suggested in zebrafish (Yoon et al., 1997; Braat et al., 1999). To address this question, we followed germ plasm–positive cells during early embryogenesis. In the 512-cell stage embryos, dividing cells segregate the germ plasm with one of the two daughter nuclei, whereas in sphere stage (cell cycle 13) embryos, germ plasm is inherited by both daughter cells (Fig. 7, d and e). In 1,000-cell stage embryos, we still see germ plasm as a tight structure restricted to one part of the cell (Fig. 7 a). Three-dimensional analysis shows that the germ plasm is punctate and tightly localized between the nucleus and the vegetal-most membrane, often forming a cuplike structure (data not shown). Beginning at the sphere stage (cell cycle 12–13) the germ plasm disintegrates and seems to spread into the cytoplasm (Fig. 7 b). Shortly before gastrulation (30% epiboly), the germ plasm is fully disintegrated and fills the cytoplasm evenly in little patches (Fig. 7 c).

Germ plasm is localized to one side of the division plane during early cell divisions, as seen in centriole and microtubule double stainings for cell polarity (Fig. 7 f and data not shown). Most frequently, we see the axis of cellular division to the animal-vegetal axis with the germ plasm segregated to the vegetal spindle pole. Therefore, the observed low number of *vasa*-positive cells in early embryogenesis is due to asymmetric localization of germ plasm to one daughter cell, which is a process that is discontinued at the beginning of the sphere stage (cell cycle 12–13) when germ plasm fills the cytoplasm. In addition, changes in the germ plasm segregation pattern are observed before the beginning of Vasa protein localization and zygotic *vasa* transcription, suggesting that this change is independent of Vasa protein function.

Germ Plasm Localization and Segregation Is Impaired in Maternal Nebel Mutants

Since initial *vasa* RNA segregation along the first two cellular cleavages is impaired in *nebel* mutant embryos, we were interested whether the *nebel* mutation affects germ plasm integrity and possibly also asymmetric germ plasm segregation (Pelegri et al., 1999). Sectioning *nebel* mutant embryos, we find that *vasa* RNA is still localized to nuage-like structures in the 8-cell stage embryos, although the germ plasm is seen in ectopic locations close to the center of the embryos instead of its wild-type location at the distal part of the cleavage furrows (Fig. 8, a and b). Therefore, the *nebel* mutation does not affect germ plasm integrity, but affects the movement of *vasa* RNA and other germ plasm components along the forming furrow.

To investigate possible defects in unequal germ plasm segregation in *nebel* embryos, we followed *vasa* RNA as a marker of germ plasm in *nebel* embryos from the 256- to the 1,000-cell stage. We find that, in some dividing cells, the asymmetric segregation of the germ plasm is defective, so that it is distributed prematurely to both daughter cells (Fig. 8 d). This results in additional germ plasm–containing

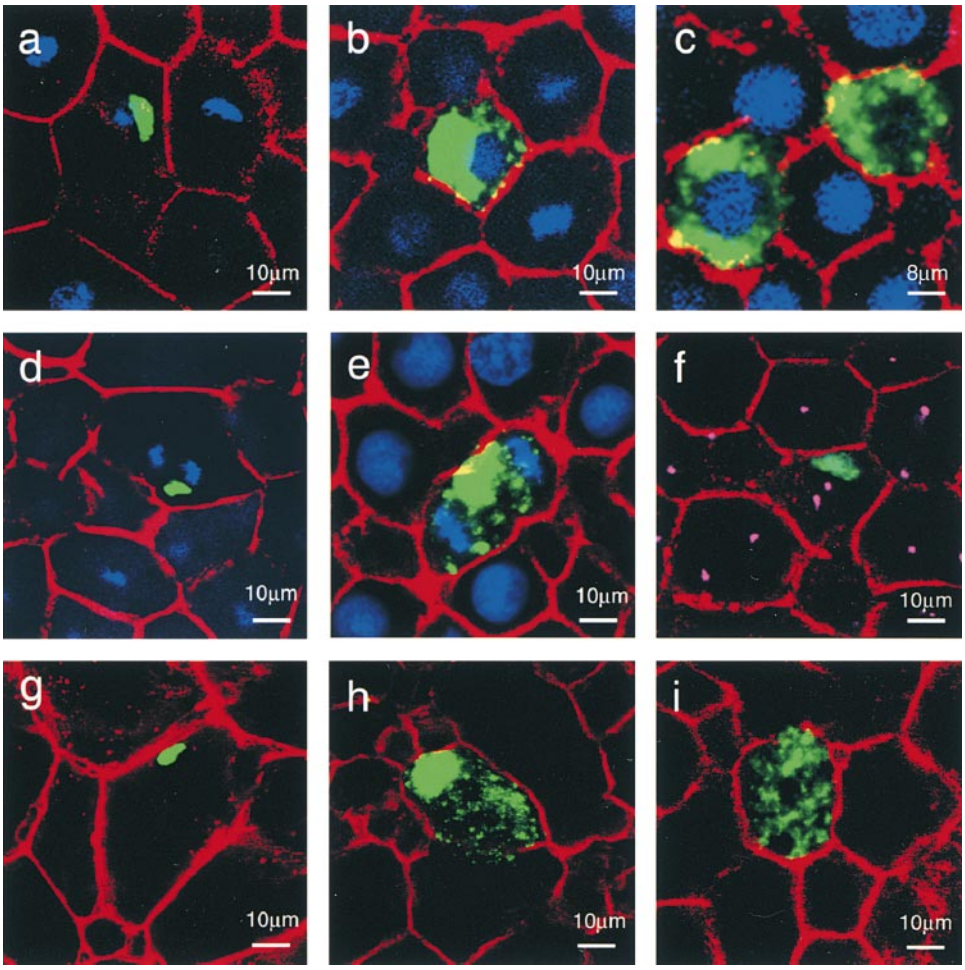

Figure 7. vasa RNA distribution during early embryogenesis. Embryos were stained for *vasa* RNA (green), β-catenin (red), DNA (blue), and γ-tubulin (pink in f only). In 1,000-cell stage embryos, the *vasa* RNA is confined to a cortical, more vegetal region (a). Beginning at the sphere stage, the tight localization of *vasa* RNA is lost and spreads into the cytoplasm (b). At 30% epiboly, the *vasa* RNA localization is lost and fills the cytoplasm in little patches (c). In the 512-cell stage embryos, dividing cells segregate *vasa* RNA to only one daughter cell (d), whereas sphere stage embryos distribute *vasa* RNA equally to daughter cells (e). During asymmetric segregation, the *vasa* RNA is always colocalizing with one of the two centrioles (f). In aphidicolin-treated embryos that lack any detectable nuclei, *vasa* RNA is localized in 1,000-cell stage embryos (g), starts to disperse into and eventually evenly fills the cytoplasm at early to late sphere stage (h and i).

cells in close proximity to their daughter cells, although they contain smaller amounts of germ plasm (Fig. 8 c). Assessing the number of *vasa* RNA–positive cells at the 1,000-cell stage in *nebel* and wild-type embryos shows that, in *nebel* embryos, on average, seven cells carry germ plasm, compared with five in wild-type (Table I). Since the *nebel* phenotype is variable, we compared the frequency of embryos with additional germ plasm–containing cells. We find that the distribution is broader in *nebel* than in wild-type embryos, and a significant proportion of *nebel* embryos carry two to three times as many cells with germ plasm as wild-type embryos (Fig. 8, e and f). Therefore, we conclude that the *nebel* mutation affects germ plasm migration both early to the distal part of furrows and later during asymmetric segregation. This suggests a common mechanism for both processes.

The Change from Asymmetric to Symmetric Germ Plasm Segregation Is Independent of Zygotic Signals and the Nucleus

We investigated whether the signals triggering the end of asymmetric *vasa* RNA segregation at the late blastula stage are dependent on nuclear signals or whether they are dependent on the cytoplasm or the germ plasm itself. To address this question, we analyzed *vasa* RNA segregation in embryos where cell division occurs but which lack nuclei. Single-cell stage embryos were treated with aphidi-

Table I. Number of Presumptive PGCs during Zebrafish Embryogenesis

Stage	1 cell	128 cell	1,000 cell	Sphere	Dome	50 percent epiboly	1 day
Total cell number	1	128	1,000	8,000	12,000	24,000	?
Average number of PGCs in wild-type*	1.0 ± 0 (n = 32)	4.0 ± 0.7 (n = 31)	5.0 ± 0.9 (n = 31)	6.1 ± 1.3 (n = 24)	10.3 ± 2.6 (n = 21)	15.1 ± 4.0 (n = 30)	29.9 ± 4.1 (n = 27)
Average number of PGCs in *nebel* mutants*‡	nd	nd	7.0 ± 1.8 (n = 36)	nd	nd	nd	31.1 ± 9.4 (n = 33)

*Sample size (n) and SD are indicated.
‡nd, nondetermined.

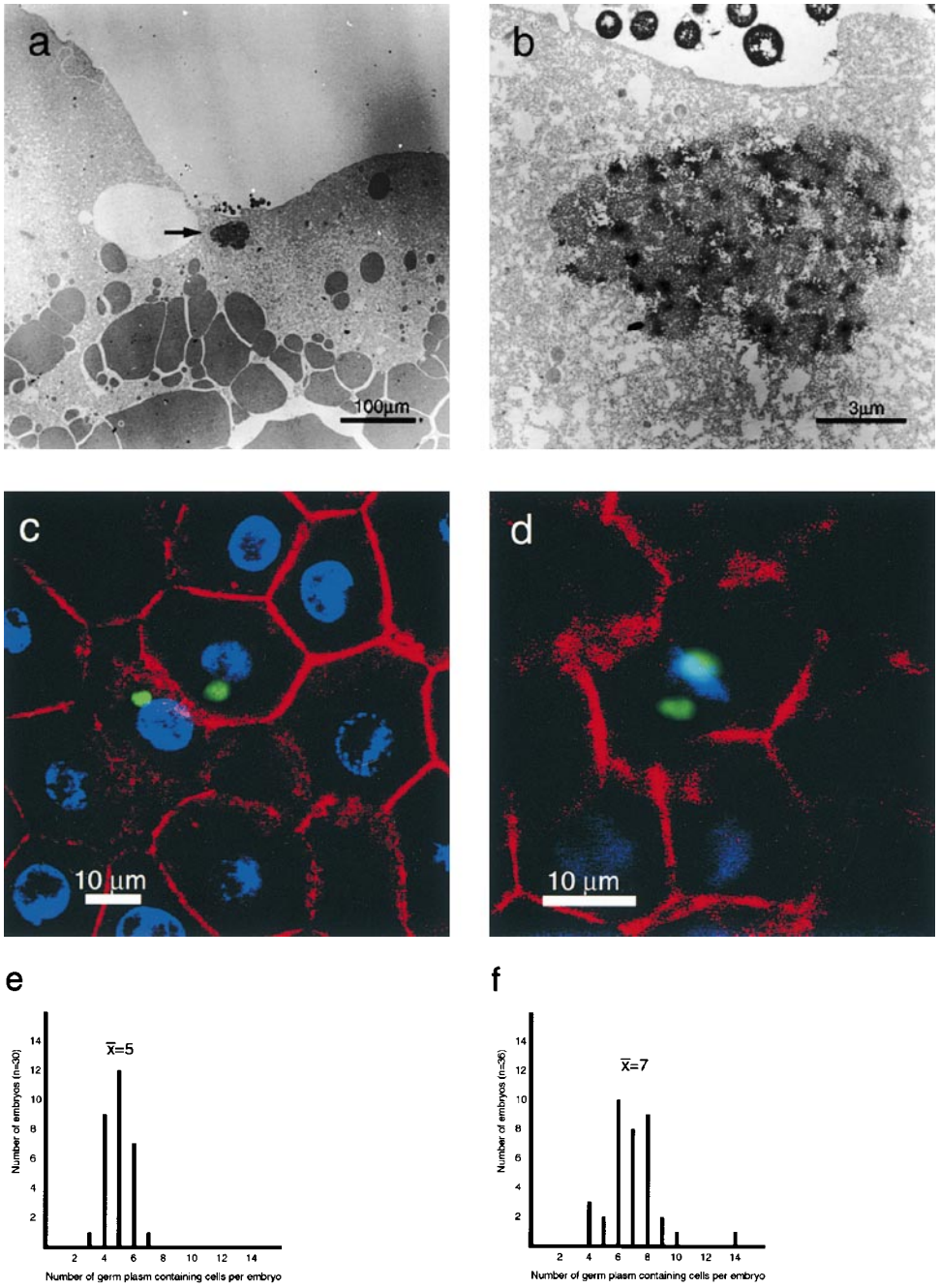

Figure 8. *vasa* RNA localization in embryos from *nebel* mutant mothers. Electron microscopy sections of eight-cell *nebel* embryos stained for *vasa* RNA. Embryos were hybridized with antisense *vasa* RNA fragments, embedded, and were processed for electron microscopy (a and b). All sections are along the animal-vegetal axis. *vasa* RNA is confined to the same structure as in wild-type (Fig. 1, a and b), although furrow indentation is impaired. For confocal analysis, embryos were stained for *vasa* RNA (green), β-catenin (red), and DNA (blue). In 512-cell stage *nebel* embryos, we often find *vasa* RNA at both sides of the division plane (d), and both daughter cells inherit *vasa* RNA (c). A comparison of *vasa* RNA segregation in wild-type (e) and *nebel* mutant embryos (f) shows that, in mutant embryos, the subpopulation of *vasa* RNA–positive cells is increased.

colin to inhibit DNA replication and, as a consequence, nuclear division (Nagano et al., 1981; Raff and Glover, 1989). Treated embryos developed until the sphere to dome stage (cell cycle 12–14), and cell division was normal as judged by centriole stainings, although few to no nuclei were detectable (data not shown). Germ plasm segregation was also unaffected in treated embryos. In the 512-cell stage embryos, germ plasm tightly localized to one part of the cell and only four to five aggregates were observed (Fig. 7 g). This localization was lost during early to the late sphere stage (cell cycle 12–13; Fig. 7, h and i). At this stage, a greater number of vasa RNA–positive cells were observed, which is consistent with the idea that the asymmetric segregation program has been completed. Similarly, we did not see any effect on germ plasm segregation in embryos treated with the transcription inhibitor actinomycin D (data not shown). These experiments show that the signal(s) that trigger the switch from asymmetric to symmetric germ plasm segregation depend neither on the nucleocytoplasmic ratio nor on the activation of zygotic gene expression.

Discussion

The Nature of the Zebrafish Germ Plasm

In this paper, we describe a nuage-like structure that contains *vasa* transcripts (Fig. 1). The structure consists of po-

rous elements embedded in electron-dense material, frequently in contact or close proximity to mitochondria and the cytoskeleton, resembling nuage structures in oocytes and 4 dpf embryos of earlier reports (Selman et al., 1993; Braat et al., 1999). We find the structure associated with *vasa* RNA in embryos up to the 1,000-cell stage, which is a time point where the structure is restricted to a subpopulation of cells that are believed to give rise to the germline (Fig. 1, a–d). Since nuage-like structures have been identified as germ plasm organelles in many species (for reviews see Eddy, 1975; Wylie, 1999) we suggest that the *vasa* RNA–containing structure is the zebrafish germ plasm. Similar observations have been reported in *Caenorhabditis*, *Drosophila*, and *Xenopus*, where nuage-like structures are associated with the germline throughout the life cycle of these animals (Mahowald, 1962, 1968, 1971; Whitington and Dixon, 1975; Wolf et al., 1983). However, in *Drosophila* and *Caenorhabditis*, the Vasa protein and its orthologues but not their corresponding RNAs are part of the polar granules/P granules (Hay et al., 1988a,b; Lasko and Ashburner, 1990; Gruidl et al., 1996). This is in contrast to zebrafish, where we find *vasa* RNA but not Vasa protein to be a component of the germ plasm (Fig. 3 f).

In *Drosophila*, Vasa protein localization to the germ plasm is dependent on localized *oskar* RNA, the key component in germ plasm assembly and abdominal patterning (Ephrussi et al., 1991; Ephrussi and Lehmann, 1992). It is tempting to speculate that localization of *vasa* RNA to germ plasm may be a vertebrate variant to restrict Vasa protein expression to the future PGCs. In *Xenopus*, the Vasa protein homologue, *Xenopus* Vasa-like gene 1, also is localized perinuclear at the onset of gastrulation (Ikenishi et al., 1996). However, as the localization pattern of the *Xenopus* Vasa-like gene 1 RNA has not been reported, it cannot be concluded whether the restriction of Vasa protein expression via the localization of *vasa* RNA is a commonly used mechanism.

Transport of Zebrafish Germ Plasm

In the 1-cell stage embryos, we see numerous small germ plasm particles in close proximity to the cortical actin mesh, sometimes also in direct physical contact. After the first and second cleavage, the germ plasm aggregates and moves to a position underneath the distal part of the cleavage furrows, where it is found in close proximity with the microtubule (Fig. 2). Disruption of the actin mesh by exposure to latrunculin B before furrow formation inhibits aggregation of cortical germ plasm particles (data not shown). A possible involvement of the actin network in these processes cannot be directly tested since actin inhibitors affect proper furrow formation. However, the colocalization of germ plasm aggregates with the actin network is suggestive of a role for this cytoskeletal network in vasa RNA recruitment at the furrow. In addition, depolymerization of the microtubule by nocodazole after furrow initiation results in a failure of germ plasm to move distally along the forming furrow (Pelegri et al., 1999). Germ plasm translocation also is impaired in *nebel* mutant embryos. Our previously reported studies attribute the loss of germ plasm movement to distal cleavage planes in both the *nebel*- and nocodazole-treated embryos to a reduction of the furrow microtubule array (FMA; Pelegri et al., 1999). These observations suggest that the initial assembly of germ plasm particles into larger aggregates at the forming furrow is actin-mediated, and that the subsequent peripheral movement of germ plasm along the cleavage plane is FMA-dependent.

The importance of the cytoskeleton for germ plasm assembly also has been shown in *Drosophila* and *Xenopus*. In *Drosophila*, the recruitment of the posterior pole plasm components is microtubule- and actin-dependent (Erdelyi et al., 1995; Pokrywka and Stephenson, 1995; Lantz et al., 1999). Flies fed on a diet supplemented with the microtubule polymerization inhibitor colchicine produce oocytes that fail to localize *oskar* RNA to the posterior pole. In wild-type flies, *oskar* RNA induces the assembly of germ plasm at the posterior pole, causing development of the abdomen and germline (Ephrussi et al., 1991; Ephrussi and Lehmann, 1992). *oskar* RNA localization to the posterior pole is also strongly reduced in tropomyosin II mutant oocytes, indicating a dependence of *oskar* RNA localization on the actin network (Erdelyi et al., 1995). In *Xenopus*, germ plasm assembly is microtubule-dependent (Ressom and Dixon, 1988). Injection of different microtubule inhibitors into activated eggs consistently abolished germ plasm aggregation, whereas actin depolymerization showed no effect on germ plasm assembly. The role of microtubules in *Xenopus* germ plasm aggregation is substantiated by the requirement of a microtubule-dependent kinesin-like protein, Xklp1 (Robb et al., 1996). Although germ plasm assembly is cytoskeleton-dependent in *Drosophila*, *Xenopus* and zebrafish, there are different temporal requirements for actin and microtubule. In *Drosophila*, pole plasm components require an intact actin and microtubule network simultaneously, whereas, in *Xenopus*, the actin network is dispensable for germ plasm aggregation. In zebrafish, the initial germ plasm aggregation may be actin-dependent, whereas the subsequent segregation requires a functional FMA.

A Change in Structure and Segregation of Germ Plasm Induces Germ Cell Specification

During zebrafish embryogenesis, cell number and diversity increase as cells divide and adopt different identities. One way to determine diverse cell fate is to partition determinants unequally between daughter cells. Such a mechanism is employed in zebrafish germline specification. During the first cell divisions, *vasa* RNA–containing germ plasm is asymmetrically segregated to four cells. During subsequent cleavage, asymmetric segregation of this aggregate results in an invariant number of four to five PGCs. At the sphere stage (cell cycle 13), these four cells begin to divide symmetrically and eventually give rise to ~30 PGCs (Table I, Fig. 7).

While presumptive PGCs divide unequally, the germ plasm colocalizes with microtubules and one of the two centrioles (Fig. 7, data not shown), suggesting a role of the spindle apparatus in asymmetric germ plasm segregation as has been proposed for *Xenopus* germ plasm segregation (Whitington and Dixon, 1975). This is in agreement with impaired asymmetric germ plasm segregation in *nebel* mutant embryos (Fig. 8), which is a maternal-effect mutation

that affects the FMA and FMA-based translocation of germ plasm in 4-cell stage embryos (Pelegri et al., 1999). However, it is also possible that this phenotype is a secondary consequence of other nebel-associated phenotypes, such as the insertion of newly added membrane (Pelegri et al., 1999). Further work will be necessary to clarify this issue.

During the transition from unequal to equal cell division in presumptive PGCs, germ plasm fills the cytoplasm and changes from a tight to a more diffuse structure. The initial signals that trigger this change are of maternal and nonnuclear origin since germ plasm structure and segregation are unaffected in embryos where DNA replication is inhibited and cell division progresses normally until early dome stages (cell cycle 13–14; Fig. 7, g–i). Furthermore, these signals need to be linked tightly to the number of cell divisions to induce relocalization of germ plasm exactly at the late sphere (cell cycle 13) stage. In *Xenopus,* the ratio of chromatin to cytoplasm has been implicated in a similar process, which is the timing of MBT (Newport and Kirschner, 1982). The chromatin/cytoplasm ratio cannot account for the timing of germ plasm relocalization in zebrafish since the chromatin level does not change in replication-inhibited embryos during development. Rather, we believe that the timing owes to an unknown counting mechanism that may be related to the germ plasm itself or other cellular processes, such as the division of the centrioles, whose division and colocalization with the germ plasm is unaffected in cells lacking nuclear DNA.

Vasa protein begins to localize around the nuclei of presumptive PGCs at about the same stage as when *vasa* RNA asymmetric segregation is lost. From this stage on, *vasa* RNA and protein are now inherited by both daughter cells. As a consequence, the number of PGCs starts to increase and we find that zygotic *vasa* transcription is initiated (Table I, Figs. 4 and 5). It is tempting to speculate that the beginning of zygotic *vasa* expression indicates a fate decision in cells that contain germ plasm to adopt a germ cell fate. This idea is supported by the fact that *vasa* homologues in *Drosophila* and *Caenorhabditis* are essential for germ cell formation and in mice for male germ cell proliferation (Hay et al., 1988b; Lasko and Ashburner, 1988; Gruidl et al., 1996; Tanaka et al., 2000). However, the inheritance of *vasa* RNA alone does not suffice to induce zygotic *vasa* transcription since injection of *vasa* mRNA into 1-cell stage embryos did not yield an increase in PGCs, the *vasa* RNA was rapidly degraded (Weidinger et al., 1999). Therefore, it is likely that additional factors, possibly residing within the germ plasm, are required to specify germ cell fate. In the absence of additional germ cell markers, it is impossible to further substantiate the suggestion that the beginning of zygotic *vasa* transcription is indicative of germ cell fate specification. Although germ plasm represses early zygotic expression in PGCs of *Drosophila* and *Caenorhabditis* (Zalokar, 1976; Seydoux and Dunn, 1997; Asaoka et al., 1998; Van Doren et al., 1998), the delayed onset of zygotic *vasa* transcription is not a consequence of transcriptional repression of germ cell nuclei. We find that transcription initiated at the MBT in all nuclei irrespective of germ plasm. In *Xenopus,* similar changes in germ plasm localization shortly before gastrulation have been suggested to reflect germ plasm activation (Whitington and Dixon, 1975). If relocalization of germ plasm in zebrafish is linked to its activation, one possible consequence of this process may be the translation of stored maternal transcripts such as *vasa* RNA. Indeed, we see weak Vasa protein signals in aphidicolin-treated embryos at the sphere stage (cell cycle 13; data not shown). This indicates that maternal *vasa* RNA is translated in the absence of zygotic transcription. Since Vasa protein is homologous to RNA helicases and is implicated in initiating translation of maternal transcripts in *Drosophila* (Styhler et al., 1998; Tomancak et al., 1998), it is tempting to speculate that newly translated Vasa protein facilitates translation of other germ cell–associated transcripts, including *vasa* RNA itself. Because the appearance of the Vasa protein also coincides with the activation of zygotic *vasa* transcription, it is also possible that protein products that are dependent on Vasa protein for their translation result in the expression of germline-specific genes and germline fate commitment. However, in the absence of *vasa* mutations in zebrafish, we cannot rule out the possibility that Vasa protein does not play a role in germ cell specification, but rather is required during later stages of germ cell development. Evidence for germ cell inducing capacity of germ plasm comes from transplantation experiments in amphibians, where it has been shown that the amount of germ plasm determines the number of PGCs. When germ plasm is successively removed, the number of PGCs decreases accordingly. Total removal of germ plasm leads to sterility (for review see Nieuwkoop and Sutasurya, 1979). In *nebel* embryos, the germ plasm is often equally instead of unequally segregated to daughter cells (Fig. 8 d). This results in more cells that carry smaller amounts of germ plasm at the 1,000-cell stage.

In summary, our observations suggest the following steps for germ cell determination in zebrafish. Unequal germ plasm partitioning separates four cells from the embryo that have the potential to form the germline. These presumptive PGCs turn into true PGCs (Whitington and Dixon, 1975) at the sphere stage (cell cycle 13) when they start expressing *vasa* RNA, a germline-specific marker. This presumptive fate commitment is preceded by the translocation of the germ plasm from its cortical to a more diffuse cytoplasmic location. The change in germ plasm localization is induced by a maternal program that is independent of the nucleocytoplasmic ratio and zygotic transcription. This maternal program results in Vasa protein localization around the nucleus and initiation of zygotic *vasa* transcription. Vasa protein accumulation may originate from maternal *vasa* RNA but is primarily dependent on zygotically derived transcripts. These events result in the expression of germline-specific markers and equal cell division that give rise to ~30 PGCs, the founder population of the germline. Upon migration to the gonads, the PGCs resume proliferation and spermatogenesis or oogenesis will begin (Yoon et al., 1997). Further analysis of maternal-effect mutants defective in *vasa* RNA segregation together with zygotic screens for germline defects will shed more light on germline formation in zebrafish.

We are grateful for the excellent technical assistance of Inge Zimmermann, Brigitte Sailer, and Birgitta Latemann for help with embedding and sectioning. We also would like to thank Hans-Martin Maischein and Kai-Erik Witte for advice and help with in vitro fertilization. Special thanks to

Frank Schnorrer for helpful suggestions and discussions. Additionally, we are grateful to Carl Neumann, Scott Holley, and Darren Gilmour for critical comments on the manuscript.

This work was supported by the Max-Planck Society. H. Knaut was supported by a Boehringer-Ingelheim predoctoral fellowship.

Submitted: 31 January 2000
Revised: 28 March 2000
Accepted: 3 April 2000

References

Andre, J., and C. Rouiller. 1957. Electron Microscopy. *Proc. Stockholm Conf.*, 1956. 162–164.

Asaoka, M., H. Sano, Y. Obara, and S. Kobayashi. 1998. Maternal Nanos regulates zygotic gene expression in germline progenitors of *Drosophila melanogaster*. *Mech. Dev*. 78:153–158.

Bobola, N., R.P. Jansen, T.H. Shin, and K. Nasmyth. 1996. Asymmetric accumulation of Ash1p in postanaphase nuclei depends on a myosin and restricts yeast mating-type switching to mother cells. *Cell*. 84:699–709.

Braat, A.K., T. Zandbergen, S. Van de Water, H.J.T. Goos, and D. Zivkovic. 1999. Characterization of zebrafish primordial germ cells: morphology and early distribution of vasa RNA. *Dev. Dynamics*. 216:153–167.

Bregman, D.B., L. Du, S. van der Zee, and S.L. Warren. 1995. Transcription-dependent redistribution of the large subunit of RNA polymerase II to discrete nuclear domains. *J. Cell Biol*. 129:287–298.

Dahm, R., C. Gribbon, R.A. Quinlan, and A.R. Prescott. 1998. Changes in the nucleolar and coiled body compartments precede lamina and chromatin reorganization during fibre cell denucleation in the bovine lens. *Eur. J. Cell Biol*. 75:237–246.

Eddy, E. 1975. Germ plasm and the differentiation of the germ cell line. *Int. Rev. Cytol.* 43:229–280.

Ephrussi, A., and R. Lehmann. 1992. Induction of germ cell formation by *oskar*. *Nature*. 358:387–392.

Ephrussi, A., L.K. Dickinson, and R. Lehmann. 1991. Oskar organizes the germ plasm and directs localization of the posterior determinant nanos. *Cell*. 66: 37–50.

Erdelyi, M., A.M. Michon, A. Guichet, J.B. Glotzer, and A. Ephrussi. 1995. Requirement for *Drosophila* cytoplasmic tropomyosin in *oskar* mRNA localization. *Nature*. 377:524–527.

Fujiwara, Y., T. Komiya, H. Kawabata, M. Sato, H. Fujimoto, M. Furusawa, and T. Noce. 1994. Isolation of a DEAD-family protein gene that encodes a murine homolog of *Drosophila vasa* and its specific expression in germ cell lineage. *Proc. Natl. Acad. Sci. USA*. 91:12258–12262.

Gevers, P., J. Dulos, H. Schipper, and L.P. Timmermans. 1992. Origin of primordial germ cells, as characterized by the presence of nuage, in embryos of the teleost fish *Barbus conchonius*. *Eur. J. Morphol*. 30:195–204.

Gruidl, M.E., P.A. Smith, K.A. Kuznicki, J.S. McCrone, J. Kirchner, D.L. Roussell, S. Strome, and K.L. Bennett. 1996. Multiple potential germ-line helicases are components of the germ-line-specific P granules of *Caenorhabditis elegans*. *Proc. Natl. Acad. Sci. USA*. 93:13837–13842.

Haffter, P., M. Granato, M. Brand, M.C. Mullins, M. Hammerschmidt, D.A. Kane, J. Odenthal, F.J. van Eeden, Y.J. Jiang, C.P. Heisenberg, et al. 1996. The identification of genes with unique and essential functions in the development of the zebrafish, *Danio rerio*. *Development*. 123:1–36.

Hamaguchi, S. 1982. A light- and electron-microscopic study on the migration of primordial germ cells in the teleost, *Oryzias latipes*. *Cell. Tissue Res*. 227: 139–151.

Hay, B., L. Ackerman, S. Barbel, L.Y. Jan, and Y.N. Jan. 1988a. Identification of a component of *Drosophila* polar granules. *Development*. 103:625–640.

Hay, B., L.Y. Jan, and Y.N. Jan. 1988b. A protein component of *Drosophila* polar granules is encoded by vasa and has extensive sequence similarity to ATP-dependent helicases. *Cell*. 55:577–587.

Hirata, J., H. Nakagoshi, Y. Nabeshima, and F. Matsuzaki. 1995. Asymmetric segregation of the homeodomain protein Prospero during *Drosophila* development. *Nature*. 377:627–630.

Hopman, A.H., F.C. Ramaekers, and E.J. Speel. 1998. Rapid synthesis of biotin-, digoxigenin-, trinitrophenyl-, and fluorochrome-labeled tyramides and their application for in situ hybridization using CARD amplification. *J. Histochem. Cytochem*. 46:771–777.

Horvitz, H.R., and I. Herskowitz. 1992. Mechanisms of asymmetric cell division: two Bs or not two Bs, that is the question. *Cell*. 68:237–255.

Ikenishi, K., T.S. Tanaka, and T. Komiya. 1996. Spatio-temporal distribution of the protein of *Xenopus vasa* homologue (*Xenopus* vasa-like gene 1, XVLG1) in embryos. *Dev. Growth Differ*. 38:527–535.

Illmensee, K., and A.P. Mahowald. 1974. Transplantation of posterior polar plasm in *Drosophila*. Induction of germ cells at the anterior pole of the egg. *Proc. Natl. Acad. Sci. USA*. 71:1016–1020.

Jan, Y.N., and L.Y. Jan. 1998. Asymmetric cell division. *Nature*. 392:775–778.

Jan, Y.N., and L.Y. Jan. 1999. Asymmetry across species. *Nat. Cell Biol*. 1:E42–44.

Kane, D.A., and C.B. Kimmel. 1993. The zebrafish midblastula transition. *Development*. 119:447–456.

Kim, E., L. Du, D.B. Bregman, and S.L. Warren. 1997. Splicing factors associate with hyperphosphorylated RNA polymerase II in the absence of pre-mRNA. *J. Cell Biol*. 136:19–28.

Kimmel, C.B., W.W. Ballard, S.R. Kimmel, B. Ullmann, and T.F. Schilling. 1995. Stages of embryonic development of the zebrafish. *Dev. Dyn*. 203:253–310.

Knoblich, J.A. 1997. Mechanisms of asymmetric cell division during animal development. *Curr. Opin. Cell Biol*. 9:833–841.

Knoblich, J.A., L.Y. Jan, and Y.N. Jan. 1995. Asymmetric segregation of Numb and Prospero during cell division. *Nature*. 377:624–627.

Komiya, T., and Y. Tanigawa. 1995. Cloning of a gene of the DEAD box protein family which is specifically expressed in germ cells in rats. *Biochem. Biophys. Res. Commun*. 207:405–410.

Komiya, T., K. Itoh, K. Ikenishi, and M. Furusawa. 1994. Isolation and characterization of a novel gene of the DEAD box protein family which is specifically expressed in germ cells of *Xenopus laevis*. *Dev. Biol*. 162:354–363.

Lantz, V.A., S.E. Clemens, and K.G. Miller. 1999. The actin cytoskeleton is required for maintenance of posterior pole plasm components in the *Drosophila* embryo. *Mech. Dev*. 85:111–122.

Lasko, P.F., and M. Ashburner. 1988. The product of the *Drosophila* gene *vasa* is very similar to eukaryotic initiation factor-4A. *Nature*. 335:611–617.

Lasko, P.F., and M. Ashburner. 1990. Posterior localization of vasa protein correlates with, but is not sufficient for, pole cell development. *Genes. Dev*. 4:905–921.

Lehmann, R., and C. Nüsslein-Volhard. 1991. The maternal gene *nanos* has a central role in posterior pattern formation of the *Drosophila* embryo. *Development*. 112:679–691.

Long, R.M., R.H. Singer, X. Meng, I. Gonzalez, K. Nasmyth, and R.P. Jansen. 1997. Mating type switching in yeast controlled by asymmetric localization of ASH1 mRNA. *Science*. 277:383–387.

Mahowald, A.P. 1962. Fine structure of pole cells and polar granules in *Drosophila melanogaster*. *J. Exp. Zool*. 228:91–97.

Mahowald, A.P. 1968. Polar granules of *Drosophila*. II. Ultrastructural changes during early embryogenesis. *J. Exp. Zool*. 167:237–261.

Mahowald, A.P. 1971. Polar granules of *Drosophila*. 3. The continuity of polar granules during the life cycle of *Drosophila*. *J. Exp. Zool*. 176:329–343.

Mullins, M.C., M. Hammerschmidt, P. Haffter, and C. Nüsslein-Volhard. 1994. Large-scale mutagenesis in the zebrafish: in search of genes controlling development in a vertebrate. *Curr. Biol*. 4:189–202.

Nagano, H., S. Hirai, K. Okano, and S. Ikegami. 1981. Achromosomal cleavage of fertilized starfish eggs in the presence of aphidicolin. *Dev. Biol*. 85:409–415.

Newport, J., and M. Kirschner. 1982. A major developmental transition in early *Xenopus* embryos. I. Characterization and timing of cellular changes at the midblastula stage. *Cell*. 30:675–686.

Nieuwkoop, P.D., and L.A. Sutasurya. 1979. Primordial Germ Cells in the Chordates. Cambridge University Press, Cambridge, London/New York/ Melbourne. 81–127.

Ober, E.A., and S. Schulte-Merker. 1999. Signals from the yolk cell induce mesoderm, neuroectoderm, the trunk organizer, and the notochord in zebrafish. *Dev. Biol*. 215:167–181.

Okada, M., I.A. Kleinman, and H.A. Schneiderman. 1974. Restoration of fertility in sterilized *Drosophila* eggs by transplantation of polar cytoplasm. *Dev. Biol*. 37:43–54.

Olsen, L.C., R. Aasland, and A. Fjose. 1997. A vasa-like gene in zebrafish identifies putative primordial germ cells. *Mech. Dev*. 66:95–105.

Patturajan, M., R.J. Schulte, B.M. Sefton, R. Berezney, M. Vincent, O. Bensaude, S.L. Warren, and J.L. Corden. 1998. Growth-related changes in phosphorylation of yeast RNA polymerase II. *J. Biol. Chem*. 273:4689–4694.

Pelegri, F., and S. Schulte-Merker. 1999. A gynogenesis-based screen for maternal-effect genes in the zebrafish, *Danio rerio*. *In* The Zebrafish: Genetics and Genomics. W. Detrich, L.I. Zon and M. Westerfield, editors. Academic Press Inc., New York. 1–20.

Pelegri, F., H. Knaut, H.M. Maischein, S. Schulte-Merker, and C. Nüsslein-Volhard. 1999. A mutation in the zebrafish maternal-effect gene *nebel* affects furrow formation and *vasa* RNA localization. *Curr. Biol*. 9:1431–1440.

Pitt, J.N., J.A. Schisa, and J.R. Priess. 2000. P granules in the germ cells of *Caenorhabditis elegans* adults are associated with clusters of nuclear pores and contain RNA. *Dev. Biol*. 219:315–333.

Pokrywka, N.J., and E.C. Stephenson. 1995. Microtubules are a general component of mRNA localization systems in *Drosophila* oocytes. *Dev. Biol*. 167: 363–370.

Pugh, G.E., P.J. Coates, E.B. Lane, Y. Raymond, and R.A. Quinlan. 1997. Distinct nuclear assembly pathways for lamins A and C lead to their increase during quiescence in Swiss 3T3 cells. *J. Cell. Sci*. 110:2483–2493.

Raff, J.W., and D.M. Glover. 1989. Centrosomes, and not nuclei, initiate pole cell formation in *Drosophila* embryos. *Cell*. 57:611–619.

Rappaport, R. 1996. Cytokinesis in Animal Cells. Cambridge University Press, Cambridge. 51–95.

Ressom, R.E., and K.E. Dixon. 1988. Relocation and reorganization of germ plasm in *Xenopus* embryos after fertilization. *Development*. 103:507–518.

Rhyu, M.S., and J.A. Knoblich. 1995. Spindle orientation and asymmetric cell fate. *Cell*. 82:523–526.

Rhyu, M.S., L.Y. Jan, and Y.N. Jan. 1994. Asymmetric distribution of numb protein during division of the sensory organ precursor cell confers distinct

fates to daughter cells. *Cell*. 76:477–491.
Robb, D.L., J. Heasman, J. Raats, and C. Wylie. 1996. A kinesin-like protein is required for germ plasm aggregation in *Xenopus*. *Cell*. 87:823–831.
Rongo, C., H.T. Broihier, L. Moore, M. Van Doren, A. Forbes, and R. Lehmann. 1997. Germ plasm assembly and germ cell migration in *Drosophila*. *Cold Spring Harb. Symp. Quant. Biol.* 62:1–11.
Schober, M., M. Schaefer, and J.A. Knoblich. 1999. Bazooka recruits Inscuteable to orient asymmetric cell divisions in *Drosophila* neuroblasts. *Nature*. 402:548–551.
Schüpbach, T., and E. Wieschaus. 1986. Maternal-effect mutations altering the anterior-posterior pattern of the *Drosophila* embryo. *Roux's Arch. Dev. Biol.* 195:302–317.
Selman, S., R.A. Wallace, A. Sarka, and X. Qi. 1993. Stages of oocyte development in the zebrafish, *Brachydanio rerio*. *J. Morphology*. 218:203–224.
Seydoux, G., and M.A. Dunn. 1997. Transcriptionally repressed germ cells lack a subpopulation of phosphorylated RNA polymerase II in early embryos of *Caenorhabditis elegans* and *Drosophila melanogaster*. *Development*. 124: 2191–2201.
Seydoux, G., and S. Strome. 1999. Launching the germline in *Caenorhabditis elegans*: regulation of gene expression in early germ cells. *Development*. 126: 3275–3283.
Shen, C.P., J.A. Knoblich, Y.M. Chan, M.M. Jiang, L.Y. Jan, and Y.N. Jan. 1998. Miranda as a multidomain adapter linking apically localized Inscuteable and basally localized Staufen and Prospero during asymmetric cell division in *Drosophila*. *Genes. Dev*. 12:1837–1846.
Sil, A., and I. Herskowitz. 1996. Identification of asymmetrically localized determinant, Ash1p, required for lineage-specific transcription of the yeast HO gene. *Cell*. 84:711–722.
Spana, E.P., and C.Q. Doe. 1995. The prospero transcription factor is asymmetrically localized to the cell cortex during neuroblast mitosis in *Drosophila*. *Development*. 121:3187–3195.
Spana, E.P., C. Kopczynski, C.S. Goodman, and C.Q. Doe. 1995. Asymmetric localization of numb autonomously determines sibling neuron identity in the *Drosophila* CNS. *Development*. 121:3489–3494.
Spector, I., N.R. Shochet, Y. Kashman, and A. Groweiss. 1983. Latrunculins: novel marine toxins that disrupt microfilament organization in cultured cells. *Science*. 219:493–495.
Styhler, S., A. Nakamura, A. Swan, B. Suter, and P. Lasko. 1998. Vasa is required for GURKEN accumulation in the oocyte, and is involved in oocyte differentiation and germline cyst development. *Development*. 125:1569–1578.
Takizawa, P.A., A. Sil, J.R. Swedlow, I. Herskowitz, and R.D. Vale. 1997. Actin-dependent localization of an RNA encoding a cell-fate determinant in yeast. *Nature*. 389:90–93.
Tanaka, S.S., Y. Toyooka, R. Akasa, Y. Katoh-Fukui, Y. Nakahara, R. Suzuki, M. Yokoyama, and T. Noce. 2000. The mouse homolog of *Drosophila vasa* is required for the development of male germ cells. *Genes Dev*. 14:841–853.
Tomancak, P., A. Guichet, P. Zavorszky, and A. Ephrussi. 1998. Oocyte polarity depends on regulation of gurken by Vasa. *Development*. 125:1723–1732.
Van Doren, M., A.L. Williamson, and R. Lehmann. 1998. Regulation of zygotic gene expression in *Drosophila* primordial germ cells. *Curr. Biol*. 8:243–246.
Wallace, R.A., and K. Selman. 1990. Ultrastructural aspects of oogenesis and oocyte growth in fish and amphibians. *J. Electron Microsc. Tech*. 16:175–201.
Warren, S.L., A.S. Landolfi, C. Curtis, and J.S. Morrow. 1992. Cytostellin: a novel, highly conserved protein that undergoes continuous redistribution during the cell cycle. *J. Cell. Sci*. 103:381–388.
Weidinger, G., U. Wolke, M. Koprunner, M. Klinger, and E. Raz. 1999. Identification of tissues and patterning events required for distinct steps in early migration of zebrafish primordial germ cells. *Development*. 126:5295–5307.
Whitington, P.M., and K.E. Dixon. 1975. Quantitative studies of germ plasm and germ cells during early embryogenesis of *Xenopus laevis*. *J. Embryol. Exp. Morphol*. 33:57–74.
Wodarz, A., A. Ramrath, U. Kuchinke, and E. Knust. 1999. Bazooka provides an apical cue for Inscuteable localization in *Drosophila* neuroblasts. *Nature*. 402:544–547.
Wolf, N., J. Priess, and D. Hirsh. 1983. Segregation of germline granules in early embryos of *Caenorhabditis elegans*: an electron microscopic analysis. *J. Embryol. Exp. Morphol*. 73:297–306.
Wylie, C. 1999. Germ cells. *Cell*. 96:165–174.
Yoon, C., K. Kawakami, and N. Hopkins. 1997. Zebrafish vasa homologue RNA is localized to the cleavage planes of 2- and 4-cell-stage embryos and is expressed in the primordial germ cells. *Development*. 124:3157–3165.
Zalokar, M. 1976. Autoradiographic study of protein and RNA formation during early development of *Drosophila* eggs. *Dev. Biol*. 49:425–437.